Biomedicine & Pharmacotherapy 151 (2022) 113090

Contents lists available at ScienceDirect

Biomedicine & Pharmacotherapy

journal homepage: www.elsevier.com/locate/biopha

Fc gamma receptor is not required for *in vivo* processing of radio- and drug-conjugates of the dead tumor cell-targeting monoclonal antibody, APOMAB®

Alexander H. Staudacher [a,b,*], Vasilios Liapis [a], Nicole L. Wittwer [a], William Tieu [b,c], Hiu Chun Lam [c], Jeanette Leusen [d], Michael P. Brown [a,b,e]

[a] Translational Oncology Laboratory, Centre for Cancer Biology, SA Pathology and University of South Australia, Adelaide, SA 5000, Australia
[b] School of Medicine, University of Adelaide, Adelaide, SA 5000, Australia
[c] Molecular Imaging and Therapy Research Unit, South Australian Health and Medical Research Institute (SAHMRI), Adelaide, SA 5000, Australia
[d] Immunotherapy Laboratory, Center for Translational Immunology, University Medical Center Utrecht, Utrecht, The Netherlands
[e] Cancer Clinical Trials Unit, Royal Adelaide Hospital, Adelaide, SA 5000, Australia

ARTICLE INFO

Keywords:
NOTAM
FcγR
APOMAB
ChDAB4
Zirconium-89
PBD dimer

ABSTRACT

The Fc region of a monoclonal antibody (mAb) can play a crucial role in its biodistribution and therapeutic activity. The chimeric mAb, chDAB4 (APOMAB®), which binds to dead tumor cells after DNA-damaging anti-cancer treatment, has been studied pre-clinically in both diagnostic and therapeutic applications in cancer. Given that macrophages contribute to the tumor accumulation of chDAB4 and its potency as an antibody drug conjugate *in vivo*, we next wanted to determine whether the Fc region of the chDAB4 mAb also contributed. We found that, regardless of prior labeling with chDAB4, dead EL4 lymphoma or Lewis Lung (LL2) tumor cells were phagocytosed equally by wild-type or Fcγ knock-down macrophage cell lines. A similar result was seen with bone marrow-derived macrophages from wild-type, Fcγ knock-out (KO) and NOTAM mice that express Fcγ but lack immunoreceptor tyrosine-based activation motif (ITAM) signaling. Among EL4 tumor-bearing wild-type, Fcγ KO or NOTAM mice, no differences were observed in post-chemotherapy uptake of ^{89}Zr-labeled chDAB4. Similarly, no differences were observed between LL2 tumor-bearing wild-type and Fcγ KO mice in post-chemotherapy uptake of ^{89}Zr-chDAB4. Also, the post-chemotherapy activity of a chDAB4-antibody drug conjugate (ADC) directed against LL2 tumors did not differ among tumor-bearing wild-type, Fcγ KO and NOTAM mice, nor did the proportions and characteristics of the LL2 tumor immune cell infiltrates differ significantly among these mice. In conclusion, Fc-FcγR interactions are not essential for the diagnostic or therapeutic applications of chDAB4 conjugates because the tumor-associated macrophages, which engulf the chDAB4-labelled dead cells, respond to endogenous 'eat me' signals rather than depend on functional FcγR expression for phagocytosis.

1. Introduction

Monoclonal antibody (mAb) therapy has revolutionized the field of cancer treatment by affording more targeted approaches for cancer treatment irrespective of whether the applications are diagnostic, therapeutic or theranostic. A theranostic application uses a single agent for diagnosis and to guide therapy. A mAb comprises two major parts: the fragment antigen-binding (Fab) region and the fragment crystallizable (Fc) region. The Fab region targets the antigen of interest, and it may act as an agonistic or antagonistic binder. The Fc region mediates the effector functions of a mAb and may induce immunologic responses including antibody-dependent cellular cytotoxicity (ADCC), complement-dependent cytotoxicity (CDC) and antibody-dependent cellular phagocytosis (ADCP).

The Fc region of an antibody is bound by Fc receptors (FcR) on immune cells such as lymphocytes, macrophages, and mast cells. FcR are divided into separate classes, with Fc-gamma receptors (FcγR) binding immunoglobulin G (IgG) antibodies. All FDA-approved antibody therapeutics are of the IgG class [1]. In cancer therapy, either or both the Fab and Fc regions of antibodies can mediate biologic effects *via* the

* Correspondence to: Translational Oncology Laboratory, Centre for Cancer Biology, Level 9 University of South Australia Bradley Building, North Terrace, Adelaide 5000, Australia.
E-mail address: alex.staudacher@sa.gov.au (A.H. Staudacher).

https://doi.org/10.1016/j.biopha.2022.113090
Received 7 March 2022; Received in revised form 26 April 2022; Accepted 4 May 2022
Available online 11 May 2022
0753-3322/© 2022 The Author(s). Published by Elsevier Masson SAS. This is an open access article under the CC BY-NC-ND license (http://creativecommons.org/licenses/by-nc-nd/4.0/).

promotion or blockade of intracellular signaling cascades, the induction of immune-mediated cell death, or both. Conversely, some antibodies may have no effector function or have been genetically silenced to diminish any downstream immunologic responses [2,3]. Furthermore, for the treatment of cancer, mAbs can be used as vehicles to deliver targeted therapies, such as proteins, drugs, or radiation directly to the tumor site. Here, direct interaction with the target cell can result in internalization of the complex to release the therapeutic compound. However, it is becoming clear that other non-tumor cell types can contribute to the effectiveness of therapeutic antibodies either unarmed or armed as conjugates with drugs or radionuclides [4–8].

Indeed, Li and colleagues were the first to show that tumor-associated macrophages (TAMs) can interact with ADC molecules even in the absence of target antigen binding [5]. They discovered that a non-targeting isotype control human IgG1-ADC bound to TAMs *in vivo* and exhibited similar antitumor activity to that of the therapeutic targeting ADC. This effect was only observed if the non-targeting control ADC contained a cell-permeant cytotoxin that can kill bystander cells. Moreover, Li et al. demonstrated that mutating the Fc region of the IgG1 antibody in the non-targeting control ADC to prevent binding of FcγRI and FcγRIV also abrogated its antitumor activity [5,6]. Hence, interactions between the Fc region of an ADC containing a membrane permeable payload and an FcγR molecule on TAMs result in internalization of the ADC and its processing by macrophages that is sufficient to release lethal concentrations of free cytotoxin within the tumor microenvironment [5].

The DAB4 (APOMAB®) mAb binds to La/SSB, a ribonuclear protein which only becomes exposed for antibody binding in dead and dying cells. During apoptosis, the C-terminal nuclear localisation sequence of La/SSB is cleaved, resulting in translocation of La/SSB to the cytoplasm [9,10]. La/SSB becomes available for antibody binding because of loss of cell membrane integrity in post-apoptotic necrotic cells [11]. This event permits concentrated intracytoplasmic binding of the antibody, although antibody binding to La/SSB on blebs at the apoptotic cell surface [12–15] cannot be excluded. Since La/SSB is overexpressed by many cancers, DAB4 binds specifically to tumor cells that have died after such DNA-damaging cancer treatments as ionizing radiation and certain cytotoxic chemotherapeutic drugs [16]. We have made these findings *in vitro* and *in vivo*, and shown that DAB4 can be used as a diagnostic agent to predict cancer treatment responses and as antibody conjugate therapies delivering β- and α-emitting radionuclides or highly potent cytotoxic drugs, which both mediate anti-cancer activities *via* bystander killing mechanisms [11,17–28]. We have shown that intratumoral processing of chimeric DAB4 (chDAB4) antibody conjugates results in tumor residualization of the positron-emitting radionuclide Zirconium-89 (^{89}Zr) and antitumor activity of chDAB4 antibody drug conjugates (ADC), which contain a cleavable linker and diffusible membrane-permeable drug payload, and that both effects were in part due to TAMs [21,22,27]. More recently, ^{89}Zr-labeled chDAB4, which has attenuated effector functions because of the K322A mutation in its Fc region [3], has entered clinical trials as a medical imaging agent in cancer patients (Australian New Zealand Clinical Trials Registry ID: ACTRN12620000622909) [28].

Given that the chDAB4 mAb contains a human IgG1 Fc and macrophages express FcγR, we wished to extend our findings and identify whether Fc-FcγR interactions were essential for the intratumoral processing of chDAB4 and thus the diagnostic and therapeutic activities of chDAB4 antibody conjugates. For *in vitro* studies, we used Fcγ knockdown (KD) macrophage cell lines to abrogate surface FcR expression. For *in vivo* studies, we used Fcγ knockout (KO) mice, which lack surface expression of activating FcR, and NOTAM mice. NOTAM mice are bred on an Fcγ KO background and have been genetically modified to express the human FcγR signaling chain carrying inactivating mutations of the immunoreceptor tyrosine-based activation motif (ITAM). Therefore, these mice express physiological levels of FcγR molecules which contain non-signaling human γ-chains and hence, FcγR binding to myeloid cells occurs in the absence of signal transduction [29]. In tumor-bearing mice of wild-type, Fcγ KO, or NOTAM genotypes, we examined the biodistribution of chDAB4 labelled with ^{89}Zr, after a single dose of cytotoxic chemotherapy. We also analyzed the antitumor effects of chDAB4-ADC therapy with chemotherapy in these tumor-bearing mice of different genotypes.

2. Material and methods

2.1. Cell culture

The murine RAW264.7 and J774A.1 macrophage lines, the murine Lewis lung (LL2) carcinoma line and the human Burkitt's lymphoma Raji line were purchased from Cellbank, Australia. EL4 murine thymic lymphoma cells were purchased from American Type Cell Culture (ATCC). All lines were cultured in RPMI-1640 (Sigma-Aldrich) with 5% FCS (Bovogen Biologicals). Cell lines were checked for mycoplasma contamination using MycoAlert Mycoplasma Detection Kit (Lonza) and were mycoplasma negative.

2.2. Fcγ knock-down macrophage cell lines and bone marrow derived macrophages

Control (CGCGATAGCGCGAATATATT) and *Fcer1g*-targeting (CCGCAGCTCTGCTATATCC) CRISPR plasmids of LV01 backbone were purchased from Sigma-Aldrich. Plasmids were combined with lentiviral packaging plasmids (Gag/Pol, Rev and VSVG), transfected into HEK293T cells and viral supernatant was collected 2 days later and filtered through a 0.22 μm syringe filter. Viral supernatant was spun onto Retronectin-coated 24 well plates, followed by 10^5 macrophage cells. Transduced cells were selected with 2 μg/mL puromycin in media. Bone marrow (BM) cells were flushed from the femurs of wild-type, Fcγ KO or NOTAM mice and were cultured in RPMI with 10% FCS and 20 ng/mL M-CSF (Sino Biological) for 7 days before use in experiments. Cells were screened for FcγR expression using APC-CD64 (FcγRI) and FITC-CD16.2 (FcγRIV) antibodies (Biolegend).

2.3. Chimeric DAB4

Production of chimeric DAB4 (chDAB4) has been described previously [21]. The chDAB4 mAb harbors a lysine to alanine mutation at amino acid 322 (K322A) in the CH2 domain of the Fc of human IgG1, which significantly decreases its binding to C1q and activation of complement [3].

2.4. Phagocytosis assay

LL2 or EL4 cells, which had been killed by incubation with 20 μg/mL cisplatin for 2 days, were collected, washed, and stained with CFSE or CellTrace Far Red (ThermoFisher) following manufacturer's instructions. Cells were also incubated with 10 μg/mL chDAB4 or cetuximab as a control for 20 min followed by washing and co-cultured with RAW264.7 or J774A.1 cells at a ratio of 2:1 for 1 h at 37 °C or 4 °C as a control. As a positive control, Raji cells were incubated with 10 μg/mL rituximab or cetuximab as a negative control, for 1 h at 37 °C. Both rituximab and cetuximab are chimeric mAbs containing the Fc of human IgG1. The monolayers were washed, cells collected, stained with BB515-F480 (BD Biosciences) or APC-CD11b (Biolegend) and analyzed by flow cytometry using an Accuri C6 Plus flow cytometer (BD Biosciences).

2.5. Radiolabeling and drug conjugation of chDAB4

^{89}Zr oxalate was produced *via* proton irradiation of a ^{89}Y target using a PETtrace 880 cyclotron (GE Healthcare) and purified on an Alceo Solid Target Processing system (Comecer) at the Molecular Imaging and Therapy Research Unit (MITRU), SAHMRI as previously described [30].

chDAB4 was conjugated with H_3DFOSqOEt (DFOSq) and radiolabeled with ^{89}Zr as previously described [27,31].

To create the chDAB4-ADC referred to as chDAB4-SG3249, conjugation of MA-PEG8-VA-PAB-SG3199 to chDAB4 was performed by Levena Biopharma (USA), resulting in a drug to antibody ratio of 2.8:1. The ADC was aliquoted and frozen at − 80 °C until required.

2.6. Animal experiments and treatments

All animal experiments were approved by the SAHMRI and University of South Australia Animal Ethics Committees and conducted following institutional guidelines. Breeding pairs of Fcγ KO [32] and NOTAM [29] mice, which have C57BL/6 genetic background, were provided by Prof. Leusen (University Medical Center Utrecht, Netherlands) and breeding colonies were established at the Bioresources facility of SAHMRI. Mice were genotyped for Fcγ by PCR as previously described [32] and human Fcγ was detected in Fcγ KO mice using forward and reverse primers CACATGTTCCCTACTGGTCCTC and GCACCATTGAGCACTTTATCCAC, respectively, with this PCR genotyping performed at the Garvan Institute of Medical Research, NSW. Genotyping results were confirmed by flow cytometry using peripheral whole blood samples collected from mice and stained with FITC anti-mouse FcγRIV (Biolegend), PerCP anti-mouse Ly-6 G (Biolegend) and APC anti-mouse CD11b (Biolegend), followed by red blood cell lysis.

Female wild-type, Fcγ KO or NOTAM C57Bl/6 mice were inoculated subcutaneously in the right flank with 10^6 syngeneic EL4 or LL2 cells in PBS. Mice were monitored daily using a clinical record sheet and body weight and tumor volume were measured at least 3 times per week. The tumor size was measured using electronic calipers and tumor volume was determined using the calculation: tumor volume = $(a^2 \times b)/2$, where a is the shortest diameter and b is the longest diameter of the tumor. One week later, EL4 tumor-bearing mice received intraperitoneal injections of 25 mg/kg cyclophosphamide (Baxter) and 19 mg/kg etoposide (Link Medical Products) and LL2 tumor-bearing mice received intravenous injections of 50 mg/kg gemcitabine (Hospira) and 2.5 mg/kg cisplatin (Hospira) and 50 mg/kg gemcitabine the following day. The day after chemotherapy, mice received an intravenous injection of ^{89}Zr-chDAB4 (5.5–7 MBq/20–30 μg per mouse) or 3 mg/kg chDAB4-SG3249.

2.7. In vivo bioluminescence imaging (BLI) and PET scanning

Mice were injected intraperitoneally with 100 μL of 150 mg/kg D-Luciferin (ThermoFisher), anesthetized with isoflurane and imaged using an IVIS® Spectrum Imaging system (PerkinElmer). Images were acquired for 1–30 s (representative images are shown as 1 s acquisitions 20 min following D-Luciferin injection) and the photon emissions transmitted from mice were captured and quantified as photons/sec/cm^2 using Living Image software (Version 4.7.2, Perkin Elmer).

For PET imaging, mice were anesthetized with isoflurane and scanned for 5 min using the Albira Si PET-SPECT small animal scanner (Bruker). Using the PMOD imaging suite (PMOD technologies version 4.2, Switzerland), regions of interest were manually drawn around the tumor from the Maximum Intensity Projection (MIP) sections assisted by the automatic 3D setting in PMOD software. Tumor margins and thresholds were automatically detected by the software, which includes a standardized cut off determined by PMOD, and decay corrected. At the completion of imaging, mice were humanely killed by cervical dislocation, and organs were removed, weighed and radiation counts were measured using a gamma-counter (Hidex) with background and decay corrections made.

2.8. Tumor analysis

LL2 tumors were prepared as single cell suspensions using the mouse tumor dissociation kit and GentleMACS Octo Dissociator (Miltenyi Biotec) following manufacturer's instructions. Red blood cell lysis was performed on single tumor cell suspensions as per manufacturer's instructions (eBioscience). The single tumor cell suspensions were stained with anti-CD45 BUV395, anti-I-A/I-E BV480, anti-CD11b BB515, anti-CD11c BV711, anti-F4/80 PE, anti- Ly6G and Ly6C (Gr-1) APC antibodies (BD Biosciences) following manufacturer's instructions for detection of CD45-positive cells, dendritic cells, neutrophils, and macrophages. The single tumor cell suspensions were stained with anti-CD3e BUV395, anti-CD49b Pan-NK Cells BV421, anti-CD8A PE-Cy7, anti-CD4 BV786 antibodies (BD Biosciences) following manufacturer's instructions for detection of CD3 T-cells, CD4 T-cells, CD8 T-cells, NK cells and NKT cells. Fixed Viability Stain 700 (FVS700, BD Biosciences) was used to exclude dead cells. Flow cytometric data was acquired using a BD LSR Fortessa cell analyzer (BD Biosciences) and analysis of flow cytometry data was performed using FCS Express software (De Novo Software).

2.9. Statistical analysis

Statistical analyses were performed using GraphPad Prism (v9.0) software. Comparison of two groups was performed by two-way *t*-test or intergroup comparisons made by two-way analysis of variance (ANOVA). Data are shown as mean ± standard error of the mean for biological replicates. Statistical significance was reached when $p < 0.05$, with * representing $p < 0.05$, * * representing $p < 0.01$ and * ** representing $p < 0.001$.

3. Results

3.1. Knockdown of Fcγ in macrophage cell lines does not alter phagocytosis of dead cancer cells labelled with chDAB4

CRISPR-mediated knock down of Fcγ expression was achieved in two mouse macrophage cell lines using lentiviral infection and puromycin selection. A reduction in the expression of FcγRI and FcγRIV, which are the two murine receptors shown to have the highest affinity for human IgG1 [33], was confirmed by flow cytometry (Fig. 1A). To determine whether the knocked down expression was associated with altered biologic function of these macrophages, a cell binding assay was performed using CD20$^+$ Raji cells, which were coated with the CD20-specific mAb, rituximab, or the EGFR-specific negative control mAb, cetuximab, and co-cultured with control (WT) or Fcγ KD macrophages (Fig. 1B). For both macrophage lines, the extent of binding of antibody-bound Raji cells to macrophages was significantly decreased in Fcγ KD macrophages, confirming that the reduced expression of FcγR corresponded to a reduction in antibody binding capacity.

3.2. Knockdown or knockout of Fcγ in macrophage cell lines does not alter phagocytosis of chDAB4-bound dead tumor cells by macrophages in vitro

We wished to determine whether the Fcγ KD macrophages generated above had altered capacity for phagocytosing dead, chDAB4-bound cancer cells. To determine this, EL4 or LL2 cells were killed with cisplatin for 48 h, followed by labeling with CFSE as previously described [21] and then labeling with chDAB4 or control antibody (cetuximab). The co-cultures were incubated for 1 h at 37 °C or at 4 °C as a control to limit phagocytosis, followed by washing off the dead cells. The percentage of phagocytosing macrophages was determined by flow cytometry as CD11b or F4/80 positive and CFSE positive.

The CRISPR control (Ctrl) macrophages phagocytosed both dead LL2 and EL4 cells to the same extent, regardless of whether they had been incubated with the control, non-binding antibody (cetuximab) or chDAB4 (Fig. 2). Knocking down Fcγ did not alter the phagocytosis of control- or chDAB4-labeled dead tumor cells for either macrophage line, and incubation at 4 °C abolished phagocytosis by macrophages (Fig. 2).

To confirm these results, macrophages were generated from the bone

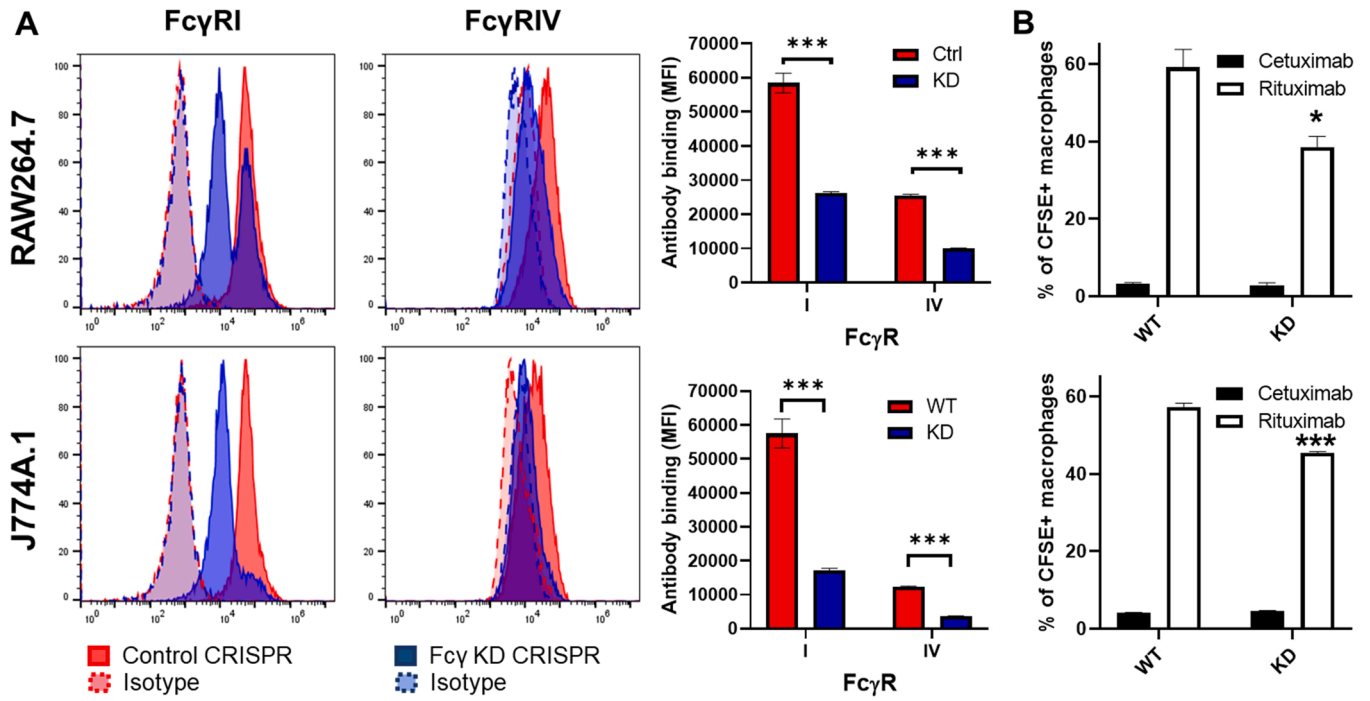

Fig. 1. Knock-down of FcγR expression in macrophage cells reduces antibody-dependent cell binding. (A) The expression of FcγRI and IV (minus isotype MFI) was examined in RAW264.7 (top row) and J774A.1 (bottom row) cells, which were infected with a lentiviral expression control plasmid (WT) or Fcγ CRISPR plasmid (KD) and selected with puromycin. (B) The extent of binding of these macrophages to CFSE-labelled Raji cells, pre-incubated with rituximab or cetuximab (control). Significant differences compared to WT macrophages incubated with rituximab-labelled Raji cells. n = 3.

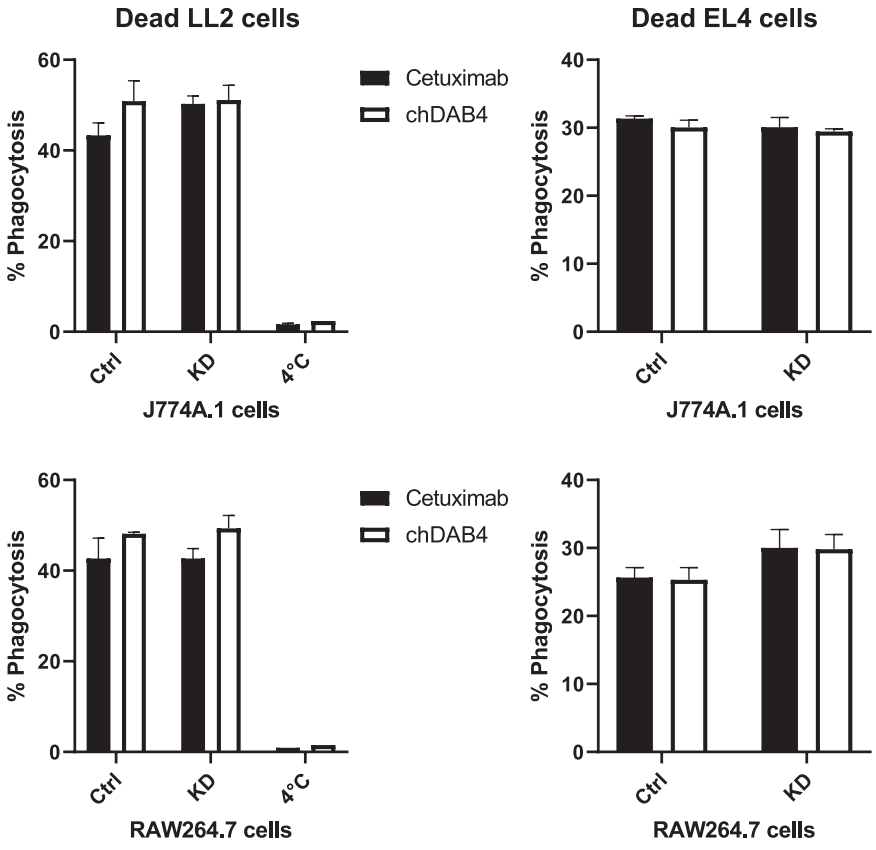

Fig. 2. J774A.1 and RAW274.7 macrophage cell lines phagocytose dead tumor cells independently of Fcγ expression status and chDAB4 labeling. J774A.1 (top row) or RAW264.7 (bottom row) cells infected with control CRISPR (Ctrl) or Fcγ CRISPR (KD) plasmids were incubated with dead LL2 (left) or dead EL4 (right) cells, which had been pre-incubated with control antibody (cetuximab) or chDAB4. Control macrophages were incubated with target cells at 4 °C to inhibit phagocytosis. The percentage of phagocytosis by the macrophages was measured. n = 3.

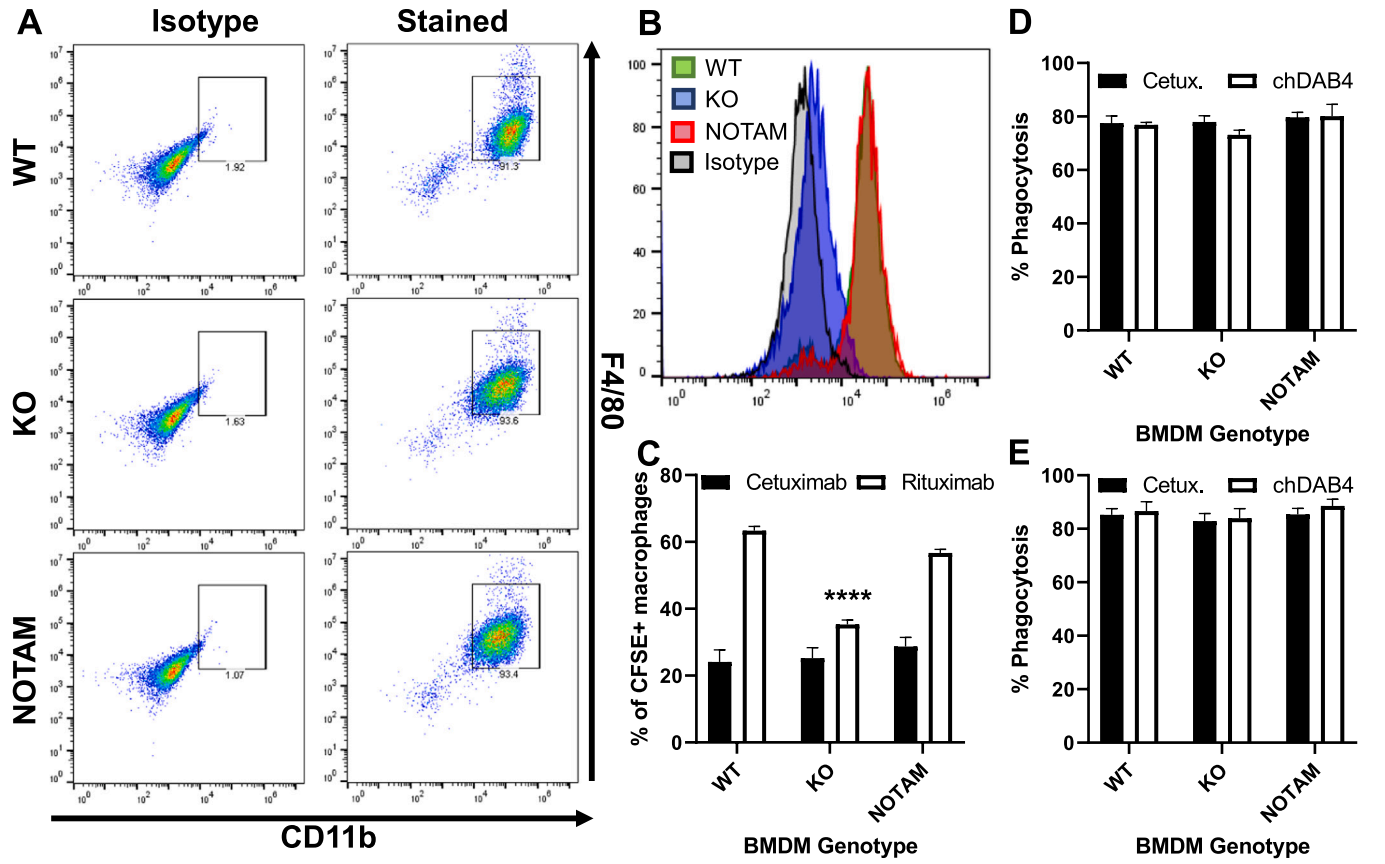

Fig. 3. Bone marrow-derived macrophages (BMDM) phagocytose dead tumor cells independently of DAB4 labeling and FcγR expression status. (A) Macrophages ($CD11b^+$ $F4/80^+$) were generated from BM of wild-type (WT), Fcγ knock-out (KO) and NOTAM mice, with (B) FcγRI expression analysis confirming lack of expression in KO BMDM but retained expression in NOTAM BMDM. (C) The binding capacity of BMDM derived from WT, Fcγ KO and NOTAM mice was examined using $CD20^+$ Raji cells labeled with rituximab or cetuximab (control). Significant difference compared to WT macrophages incubated with rituximab-labelled Raji cells. The phagocytic capacity of the BMDMs was analyzed using (D) dead EL4 and (E) dead LL2 tumor cells, which had been labeled with chDAB4 or cetuximab (control); n = 3–4.

marrow of wild-type, Fcγ KO, and NOTAM mice (Fig. 3A). NOTAM mice have a Fcγ KO background and have been genetically engineered to express human FcγR with inactivated ITAM, which allows for binding to FcγR but without downstream intracellular signaling [29]. Hence, expression of FcγRI is abrogated in bone marrow-derived macrophages (BMDM) of Fcγ KO but not of NOTAM mice (Fig. 3B).

Fcγ KO BMDM had significantly reduced binding of rituximab-opsonized Raji cells compared to wild-type BMDM, which was not evident in NOTAM BMDM (Fig. 3C). However, there was no significant difference in the phagocytosis of dead EL4 (Fig. 3D) or LL2 (Fig. 3E) tumor cells among the three genotypes, with no differences among the tumor cells pre-incubated either with control antibody (cetuximab) or chDAB4 before the co-culture. These results show that macrophage cell lines and primary macrophages phagocytose dead tumor cells *in vitro* regardless of opsonization with chDAB4. Therefore, the phagocytosis of dead tumor cells is independent of the presence of FcγR *in vitro*.

3.3. The tumor uptake of ^{89}Zr-labeled chDAB4 or the antitumor activity of chDAB4-ADC are not altered in Fcγ KO and NOTAM mice

To determine whether these *in vitro* findings also pertained *in vivo,* EL4 tumors were established in WT, Fcγ KO and NOTAM mice and mice were given chemotherapy to induce a marked increase in the numbers of dead tumor cells available for chDAB4 binding as previously described [24,25,27], followed by PET imaging of tumor uptake of ^{89}Zr-chDAB4. There was no difference in post-chemotherapy tumor growth delay among mice of the different genotypes (Fig. 4A), nor was there any difference in the tumor uptake of ^{89}Zr-chDAB4 over the imaging period (Fig. 4B, C). Tissue biodistribution studies conducted at the completion of the study did not reveal any significant differences among mice of the different genotypes in the uptake of ^{89}Zr-chDAB4 either by the tumor or normal tissues (Fig. 4D).

We also performed these experiments in mice bearing luciferase-expressing LL2 tumors (Fig. 5). Similarly, we saw no differences in post-chemotherapy tumor growth delay among mice of the different genotypes (Fig. 5A, C, D) and there were no significant differences in tumor uptake of ^{89}Zr-chDAB4 over the imaging period (Fig. 5B, E). At the end of the experiment, we found no significant differences in the tissue biodistribution study in the uptake of ^{89}Zr-chDAB4 by healthy tissues. However, there was a significant increase in tumor uptake of ^{89}Zr-chDAB4 in NOTAM mice compared to WT mice but not Fcγ KO mice (Fig. 5F).

We next investigated if WT, Fcγ KO, and NOTAM mice with established LL2 tumors exhibited any differences after chemotherapy followed by ADC treatment with the chDAB4 mAb conjugated *via* a cathepsin B-cleavable dipeptide linker to the pyrrolobenzodiazepine (PBD) dimer DNA minor groove binding drug, SG3199, to create chDAB4-SG3249, as we have shown previously [21,22]. At day 14, the mice were culled, and the immune profile of the tumors was analyzed (Fig. 6).

There were no significant differences in LL2 tumor growth rates among wildtype, Fcγ KO or NOTAM mice given chemotherapy then DAB4-SG3249 (Fig. 6A), nor were there any differences in final tumor weights among the mice of different genotypes (Fig. 6B). Also, there

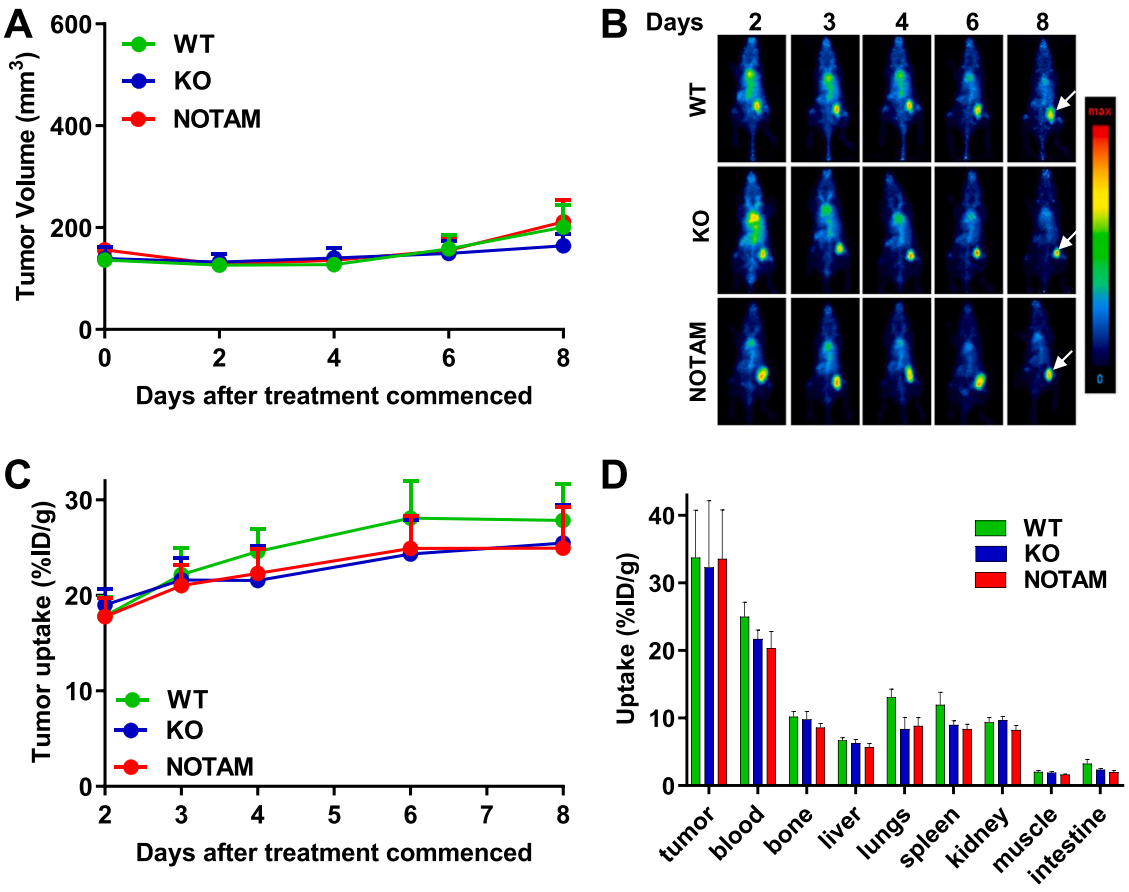

Fig. 4. Tumor uptake of 89Zr-chDAB4 in EL4 tumor-bearing mice of WT, Fcγ knock-out (KO), or NOTAM genotypes, which had been administered chemotherapy on Day 0. (A) EL4 tumor-bearing mice were given chemotherapy on Day 0 and tumor growth was measured using calipers. (B) Planar PET coronal images of mice receiving 89Zr-chDAB4 the day after chemotherapy (Day 1). Arrows indicate location of tumors. (C) Tumor uptake during the experiment measured using PMOD software and (D) tissue biodistribution at the completion of the experiment measured by physical gamma counts; n = 8 WT, n = 6 Fcγ KO, and n = 10 NOTAM mice from two independent experiments which comprised n = 6 WT, n = 4 Fcγ KO, and n = 8 NOTAM mice in the first experiment and 2 mice per group for the second experiment.

were no significant differences in the proportions of intratumoral $CD45^+$ immune and myeloid cells including macrophages, neutrophils, dendritic cells, $CD3^+$ T cells, $CD4^+$ T cells, $CD8^+$ T cells, NK cells and NKT cells between the three genotypes (Fig. 6C).

4. Discussion

In this study, using a genetic approach, we investigated the role of the IgG-binding FcγR in the processing and tumor retention of the dead tumor cell-targeting antibody, chDAB4. We used macrophage cell lines with knocked down expression of Fcγ together with BMDM from Fcγ KO and NOTAM mice to examine their ability to ingest chDAB4-labeled dead tumor cells. We also analyzed the tumor uptake of ^{89}Zr-labeled chDAB4 and the antitumor activity of a chDAB4-ADC in Fcγ KO and NOTAM mice, which had been administered chemotherapy, to determine whether the genotype of the tumor-bearing mice affected the post-chemotherapy diagnostic or therapeutic targeting behavior of the respective chDAB4 conjugates.

Fc-FcγR interactions play an important role in cancer immunotherapy, with studies showing reduced or no effectiveness of some mutant mAbs which lack FcR interactions [8] or reduced efficacy of therapeutic mAbs in Fcγ KO mice [29]. In some cases, efforts are being made to enhance the FcγR affinity of mAbs to improve their effectiveness [34]. However, this requirement depends on the mAb, tumor type and likely genetic background as to whether Fc-FcR interactions confer any additional treatment benefit [35], and in some cases abolishing FcγR interaction may result in improved outcomes [36]. Here, we wished to investigate whether Fc-FcγR interactions play any role in the phagocytosis of chDAB4-labelled dead tumor cells by macrophages, and thus whether Fc-FcγR interactions had any influence on tumor uptake of the residualizing radionuclide, ^{89}Zr [22] or the antitumor effectiveness of chDAB4-ADC therapy [21], which both depend at least partially on macrophage-mediated phagocytosis [22].

Human IgG1 binds to all human FcγR molecules [37] and human IgG molecules bind to murine FcγR with affinities similar to their binding of human FcγR, which suggests that human IgG may have similar relative FcγR-mediated biologic activities in mice [33]. However, *ex vivo* phagocytosis of antibody-opsonized erythrocytes and tumor cells does not occur with myeloid cells derived from Fcγ KO and NOTAM mice [29, 38] although it was shown that FcγR-expressing BMDM could bind antibody-opsonized tumor cells [29]. Similarly, *ex vivo* phagocytosis of antibody-opsonized particulate antigens such as bacteria was prevented in BMDM from NOTAM mice although immune complexes containing soluble antigen were internalized [39].

As expected, we found that macrophages with knocked down expression of Fcγ resulted in reduced binding of live Raji tumor cells opsonized with rituximab. However, the phagocytosis of dead tumor cells, either labeled with control antibody or chDAB4, did not change significantly compared to WT macrophages. This result was confirmed using BMDM derived from WT, Fcγ KO and NOTAM mice, showing that neither impairment of the expression nor the signaling function of FcγR altered vigorous macrophage-mediated phagocytosis of dead tumors cells, which occurred irrespective of whether the dead tumor cells had been pre-coated with chDAB4.

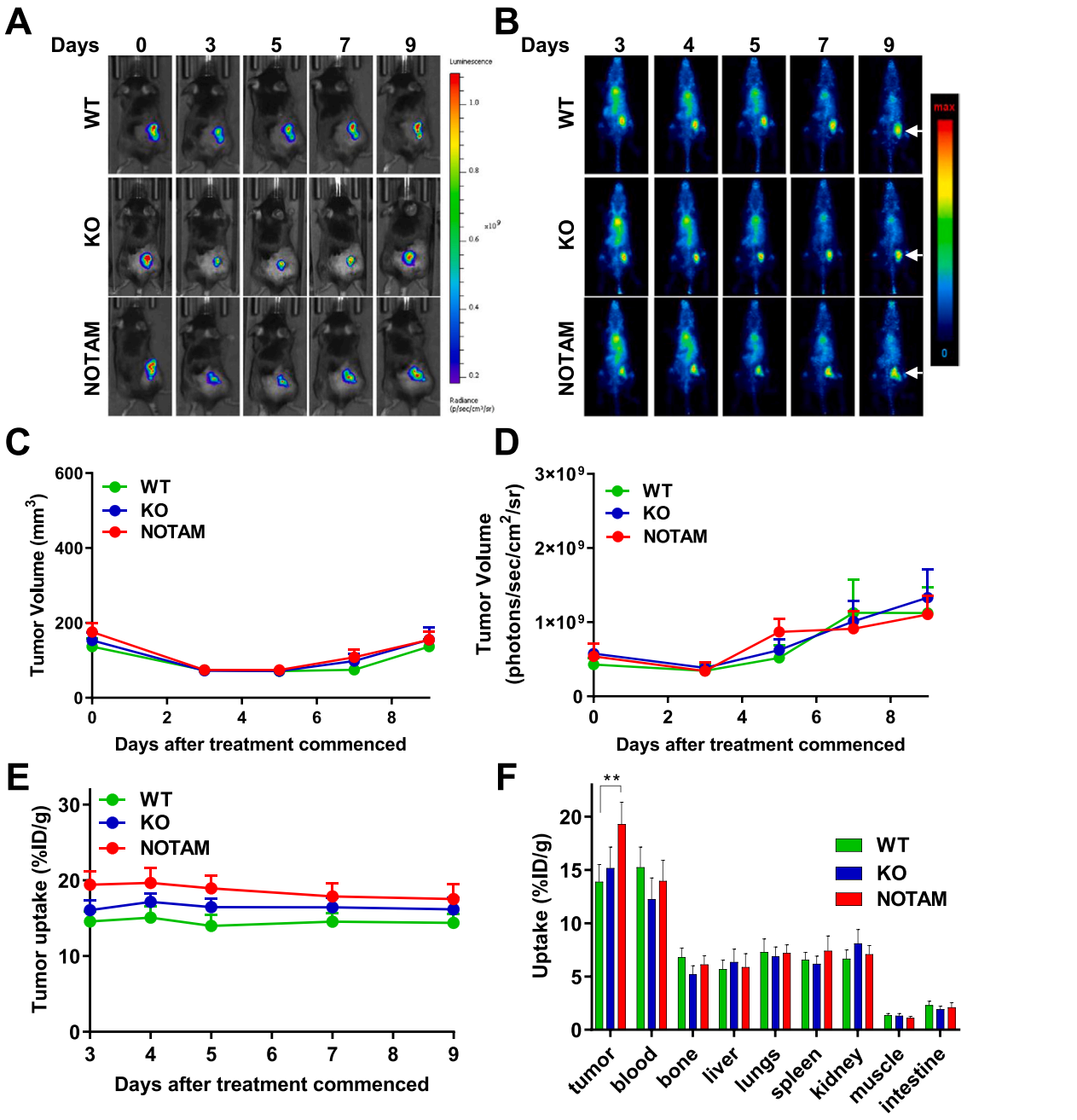

Fig. 5. Tumor uptake of ^{89}Zr-chDAB4 in LL2 tumor-bearing mice of WT, Fcγ knock-out (KO), or NOTAM genotypes, which had been administered chemotherapy. (A) Mice bearing luciferase-expressing LL2 tumors were given chemotherapy on Day 0 and 1 and tumor growth was measured using calipers (C) or an index of tumor luminescence (D). (B) Planar PET coronal images of mice receiving ^{89}Zr-chDAB4 the day after completion of chemotherapy (Day 2). Arrows indicate location of tumors. (E) Tumor uptake during the experiment measured using PMOD software and (F) tissue biodistribution at the completion of the experiment measured by physical gamma counts; n = 10 mice per genotype from three independent experiments, which comprised 5, 3 and 2 mice per group per experiment.

The post-chemotherapy tumor uptake of radioactively labelled chDAB4 was not altered among EL4 tumor-bearing mice of WT, Fcγ KO, and NOTAM genotypes. In contrast, we saw a trend towards increased post-chemotherapy tumor uptake of ^{89}Zr-chDAB4 in LL2 tumor-bearing NOTAM mice compared to WT and Fcγ KO mice by PET imaging, with a significant increase observed at completion of the study when physical γ-counts were measured in the tumors. This result may be a statistical anomaly with only one of three experiments showing a significant increase in tumor uptake in NOTAM mice (see Supplementary Fig. 1) or reflect true biologic differences between EL4 and LL2 tumors and their respective responses to anticancer treatment. For example, the EL4 tumor cell death induced by cyclophosphamide and etoposide is apoptotic, which results in the efficient phagocytic clearance of the dead cells, whereas any delays in phagocytic clearance result in mounting numbers of necrotic cells, which may be cleared less efficiently [40]. Another hypothesis to explain the difference originates from the observed trend toward higher numbers of FcγR-expressing TAMs in LL2 tumors of NOTAM mice compared to WT mice. Hence, we hypothesize that TAMs in LL2 tumors of NOTAM mice bind ^{89}Zr-chDAB4-coated dead tumor cells so that more macrophages retain surface-bound radiolabel for longer because the antibody-bound dead cells cannot be engulfed. In the absence of clearance, the antibody-bound dead cells eventually disintegrate then the ^{89}Zr-chDAB4-coated cellular debris becomes detached from binding to the FcγR molecules on TAMs when it

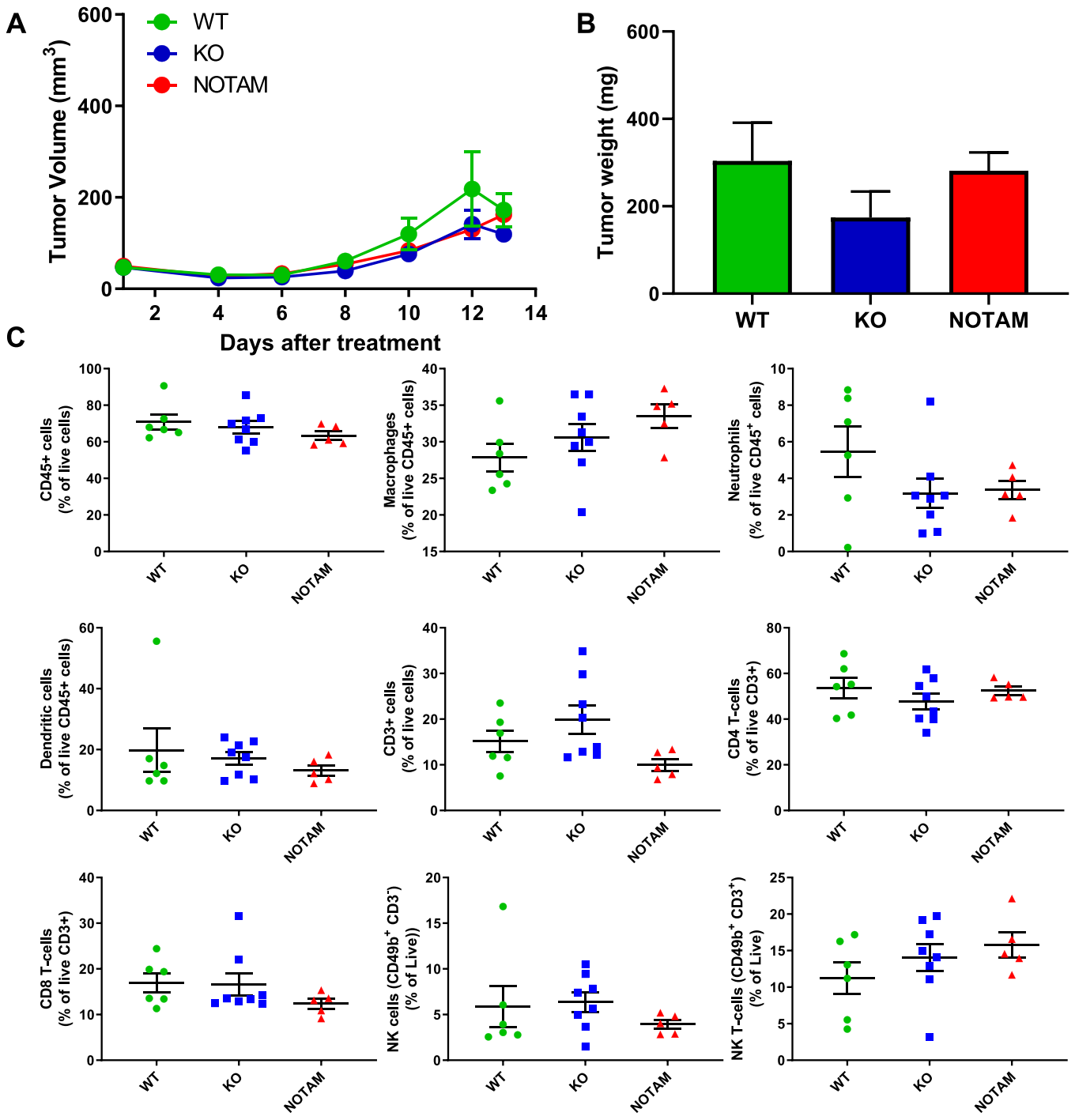

Fig. 6. Antitumor activity of sequential treatment with chemotherapy and the chDAB4-SG3249 ADC in LL2 tumor-bearing mice of wild-type, Fcγ KO, or NOTAM genotypes. Tumor-bearing mice were administered chemotherapy on Days 1 and 2 followed by chDAB4-SG3249 on Day 3 and (A) tumor growth measured by calipers. (B) Tumors weights at the end of the study. (C) Flow cytometric analyses of single cell suspensions of tumors showing the immunophenotype of infiltrates were analyzed using labeled antibodies against cell surface markers for various immune cell populations. n = 6 WT, n = 8 Fcγ KO, n = 5 NOTAM mice from a single experiment.

becomes available for phagocytosis by the same or other nearby TAMs.

Our previous data showed the critical role of TAMs in the processing of chDAB4 conjugates needed either for the detection by PET of the ^{89}Zr radiolabel retained within the tumor or the antitumor activity of the cell-permeant cytotoxin released within the tumor [22]. Others have shown that TAMs directly process ADCs *via* Fc-FcγR interactions because preventing ADC interactions with macrophage-expressed FcγR results in marked reduction of ADC effectiveness [5]. Furthermore, Fc-FcγR interactions of ADC in normal tissues can result in faster clearance and reduced effectiveness of the ADC [6]. In the case of chDAB4, Fc-FcγR was not essential because BMDM phagocytosed the target dead tumor cells, regardless of whether they were labeled with chDAB4 or not, and whether the macrophages expressed FcγR or not. The macrophages from Fcγ KO or NOTAM mice are expected to retain such other physiologic properties of macrophages as trogocytosis [38] and FcγR-independent phagocytosis of dead cells, which may explain why there was no difference in the biodistribution of chDAB4 between WT and Fcγ KO tumor-bearing mice, nor any difference in the antitumor activity of

chDAB4-ADC therapy. This effect, however, is likely to be restricted only to dead target cells, which are phagocytosed independently of FcγR because of 'eat me' signaling [41]. Conversely, although bound by NOTAM macrophages, antibody-opsonized live cells do not become internalized or are killed because of antibody-dependent cellular cytotoxicity [38,42].

In conclusion, these results show that neither the *in vitro* phagocytosis of antibody-coated dead cells nor the *in vivo* diagnostic or therapeutic activity of chDAB4 conjugates are solely dependent on Fc-FcγR interactions and, subsequently, antibody-dependent cellular phagocytosis. Moreover, these results emphasize the dominance of multiple, redundant, endogenous signals in the clearance of dead tumor cells, which thus override any requirement for Fc-FcγR interactions even though the dead tumor cells are coated with antibodies such as chDAB4.

Financial support

This work was supported by National Health and Medical Research Council, Australia (Project Grant ID 1126304), a Royal Adelaide Hospital Clinical Project Grant (Project Grant ID 12872), the Ray and Shirl Norman Cancer Research Trust, the Health Services Charitable Gifts Board (Adelaide), and AusHealth Research Pty Ltd. WT was supported through an Australian National Imaging Facility Fellowship.

CRediT authorship contribution statement

Conceptualization: **AHS, MPB**. Data curation: **AHS, VL, NW**. Formal analysis: **AHS, VL, NW, WT, MPB**, Funding acquisition: **AHS, MPB**, Investigation: **AHS, VL, NW**, Methodology: **AHS, VL, NW, WT, HCL**, Project administration: **AHS, MPB**, Resources: **AHS, WT, MPB, JL**, Validation: **AHS, VL, NW, WT, HCL, MPB**, Roles/Writing – original draft: **AHS, VL, NW, MPB**, Writing – review & editing: **AHS, VL, NW, WT, HCL, JL, MPB**,

Conflicts of interest statement

Michael P. Brown is co-inventor on APOMAB related patents owned by AusHealth Corporate Pty Ltd. No other authors have conflicts of interest to declare.

Data availability

Data will be made available on request.

Acknowledgements

This work was supported by National Health and Medical Research Council, Australia (Project Grant ID 1126304), a Royal Adelaide Hospital Clinical Project Grant (Project Grant ID 12872), the Ray and Shirl Norman Cancer Research Trust, the Health Services Charitable Gifts Board (Adelaide), and AusHealth Corporate Pty Ltd, Adelaide. WT was supported through an Australian National Imaging Facility Fellowship. The authors are grateful for the technical assistance provided by the staff in the Bioresources facility of the South Australian Health and Medical Research Institute (SAHMRI), and Dr. Wick Lakshantha (SAHMRI) for his technical assistance with PET. The graphical abstract was created using www.biorender.com.

Appendix A. Supporting information

Supplementary data associated with this article can be found in the online version at doi:10.1016/j.biopha.2022.113090.

References

[1] R.J. Brezski, G. Georgiou, Immunoglobulin isotype knowledge and application to Fc engineering, Curr. Opin. Immunol. 40 (2016) 62–69.
[2] M. Hezareh, A.J. Hessell, R.C. Jensen, J.G. van de Winkel, P.W. Parren, Effector function activities of a panel of mutants of a broadly neutralizing antibody against human immunodeficiency virus type 1, J. Virol. 75 (2001) 12161–12168.
[3] E.E. Idusogie, L.G. Presta, H. Gazzano-Santoro, K. Totpal, P.Y. Wong, M. Ultsch, Y. G. Meng, M.G. Mulkerrin, Mapping of the C1q binding site on rituxan, a chimeric antibody with a human IgG1 Fc, J. Immunol. 164 (2000) 4178–4184.
[4] A.H. Staudacher, M.P. Brown, Antibody drug conjugates and bystander killing: is antigen-dependent internalisation required? Br. J. Cancer 117 (2017) 1736–1742.
[5] F. Li, M. Ulrich, M. Jonas, I.J. Stone, G. Linares, X. Zhang, L. Westendorf, D. R. Benjamin, C.L. Law, Tumor-associated macrophages can contribute to antitumor activity through FcgammaR-mediated processing of antibody-drug conjugates, Mol. Cancer Ther. 16 (2017) 1347–1354.
[6] F. Li, M.L. Ulrich, V.F. Shih, J.H. Cochran, J.H. Hunter, L. Westendorf, J. Neale, D. R. Benjamin, Mouse strains influence clearance and efficacy of antibody and antibody-drug conjugate via Fc-FcgammaR interaction, Mol. Cancer Ther. 18 (2019) 780–787.
[7] E. Oflazoglu, I.J. Stone, K.A. Gordon, I.S. Grewal, N. van Rooijen, C.L. Law, H. P. Gerber, Macrophages contribute to the antitumor activity of the anti-CD30 antibody SGN-30, Blood 110 (2007) 4370–4372.
[8] E. Oflazoglu, I.J. Stone, L. Brown, K.A. Gordon, N. van Rooijen, M. Jonas, C.L. Law, I.S. Grewal, H.P. Gerber, Macrophages and Fc-receptor interactions contribute to the antitumour activities of the anti-CD40 antibody SGN-40, Br. J. Cancer 100 (2009) 113–117.
[9] M. Huang, H. Ida, K. Arima, H. Nakamura, T. Aramaki, K. Fujikawa, M. Tamai, M. Kamachi, A. Kawakami, H. Yamasaki, T. Origuchi, K. Eguchi, La autoantigen translocates to cytoplasm after cleavage during granzyme B-mediated cytotoxicity, Life Sci. 81 (2007) 1461–1466.
[10] K. Ayukawa, S. Taniguchi, J. Masumoto, S. Hashimoto, H. Sarvotham, A. Hara, T. Aoyama, J. Sagara, La autoantigen is cleaved in the COOH terminus and loses the nuclear localization signal during apoptosis, J. Biol. Chem. 275 (2000) 34465–34470.
[11] F. Al-Ejeh, J.M. Darby, M.P. Brown, The La autoantigen is a malignancy-associated cell death target that is induced by DNA-damaging drugs, Clin. Cancer Res. 13 (2007) 5509s–5518s.
[12] M.E. Miranda, C.E. Tseng, W. Rashbaum, R.L. Ochs, C.A. Casiano, F. Di Donato, E. K. Chan, J.P. Buyon, Accessibility of SSA/Ro and SSB/La antigens to maternal autoantibodies in apoptotic human fetal cardiac myocytes, J. Immunol. 161 (1998) 5061–5069.
[13] H.B. Tran, M. Ohlsson, D. Beroukas, J. Hiscock, J. Bradley, J.P. Buyon, T. P. Gordon, Subcellular redistribution of la/SSB autoantigen during physiologic apoptosis in the fetal mouse heart and conduction system: a clue to the pathogenesis of congenital heart block, Arthritis Rheum. 46 (2002) 202–208.
[14] L.A. Casciola-Rosen, G. Anhalt, A. Rosen, Autoantigens targeted in systemic lupus erythematosus are clustered in two populations of surface structures on apoptotic keratinocytes, J. Exp. Med 179 (1994) 1317–1330.
[15] M.E. Miranda-Carus, A.D. Askanase, R.M. Clancy, F. Di Donato, T.M. Chou, M. R. Libera, E.K. Chan, J.P. Buyon, Anti-SSA/Ro and anti-SSB/La autoantibodies bind the surface of apoptotic fetal cardiocytes and promote secretion of TNF-alpha by macrophages, J. Immunol. 165 (2000) 5345–5351.
[16] A.H. Staudacher, Y. Li, V. Liapis, M.P. Brown, The RNA-binding protein La/SSB associates with radiation-induced DNA double-strand breaks in lung cancer cell lines, Cancer Rep. (Hoboken) (2021), e1543.
[17] F. Al-Ejeh, A.H. Staudacher, D.R. Smyth, J.M. Darby, D. Denoyer, C. Tsopelas, R. J. Hicks, M.P. Brown, Postchemotherapy and tumor-selective targeting with the La-specific DAB4 monoclonal antibody relates to apoptotic cell clearance, J. Nucl. Med. 55 (2014) 772–779.
[18] S.N. Penfold, M.P. Brown, A.H. Staudacher, E. Bezak, Monte Carlo simulations of dose distributions with necrotic tumor targeted radioimmunotherapy, Appl. Radiat. Isot. 90 (2014) 40–45.
[19] A.H. Staudacher, F. Al-Ejeh, C.K. Fraser, J.M. Darby, D.M. Roder, A. Ruszkiewicz, J. Manavis, M.P. Brown, The La antigen is over-expressed in lung cancer and is a selective dead cancer cell target for radioimmunotherapy using the La-specific antibody APOMAB, EJNMMI Res 4 (2014) 2.
[20] A.H. Staudacher, E. Bezak, A. Borysenko, M.P. Brown, Targeted alpha-therapy using 227Th-APOMAB and cross-fire antitumour effects: preliminary in-vivo evaluation, Nucl. Med. Commun. 35 (2014) 1284–1290.
[21] A.H. Staudacher, Y. Li, V. Liapis, J.J.C. Hou, D. Chin, O. Dolezal, T.E. Adams, P. H. van Berkel, M.P. Brown, APOMAB antibody-drug conjugates targeting dead tumor cells are effective in vivo, Mol. Cancer Ther. 18 (2019) 335–345.
[22] A.H. Staudacher, V. Liapis, W. Tieu, N.L. Wittwer, M.P. Brown, Tumour-associated macrophages process drug and radio-conjugates of the dead tumour cell-targeting APOMAB(R) antibody, J. Control. Release 327 (2020) 779–787.
[23] F. Al-Ejeh, J.M. Darby, M.P. Brown, Chemotherapy synergizes with radioimmunotherapy targeting la autoantigen in tumors, PLoS One 4 (2009), e4630.
[24] F. Al-Ejeh, J.M. Darby, K. Pensa, K.R. Diener, J.D. Hayball, M.P. Brown, In vivo targeting of dead tumor cells in a murine tumor model using a monoclonal antibody specific for the La autoantigen, Clin. Cancer Res. 13 (2007) 5519s–5527s.
[25] F. Al-Ejeh, J.M. Darby, C. Tsopelas, D. Smyth, J. Manavis, M.P. Brown, APOMAB, a La-specific monoclonal antibody, detects the apoptotic tumor response to life-prolonging and DNA-damaging chemotherapy, PLoS One 4 (2009), e4558.

[26] B. Thierry, F. Al-Ejeh, M.P. Brown, P. Majewski, H.J. Griesser, Immunotargeting of functional nanoparticles for MRI detection of apoptotic tumor cells, Adv. Mater. 21 (2009) 541–545.
[27] V. Liapis, W. Tieu, S.E. Rudd, P.S. Donnelly, N.L. Wittwer, M.P. Brown, A. H. Staudacher, Improved non-invasive positron emission tomographic imaging of chemotherapy-induced tumor cell death using Zirconium-89-labeled APOMAB(R), EJNMMI Radio. Chem. 5 (2020) 27.
[28] V. Liapis, W. Tieu, N.L. Wittwer, T. Gargett, A. Evdokiou, P. Takhar, S.E. Rudd, P. S. Donnelly, M.P. Brown, A.H. Staudacher, Positron emission tomographic imaging of tumor cell death using zirconium-89-Labeled APOMAB(R) following cisplatin chemotherapy in lung and ovarian cancer xenograft models, Mol. Imaging Biol. 23 (2021) 914–928.
[29] S. de Haij, J.H. Jansen, P. Boross, F.J. Beurskens, J.E. Bakema, D.L. Bos, A. Martens, J.S. Verbeek, P.W. Parren, J.G. van de Winkel, J.H. Leusen, In vivo cytotoxicity of type I CD20 antibodies critically depends on Fc receptor ITAM signaling, Cancer Res. 70 (2010) 3209–3217.
[30] J.P. Holland, Y. Sheh, J.S. Lewis, Standardized methods for the production of high specific-activity zirconium-89, Nucl. Med. Biol. 36 (2009) 729–739.
[31] S.E. Rudd, P. Roselt, C. Cullinane, R.J. Hicks, P.S. Donnelly, A desferrioxamine B squaramide ester for the incorporation of zirconium-89 into antibodies, Chem. Commun. (Camb.) 52 (2016) 11889–11892.
[32] M.J. van Vugt, I.A. Heijnen, P.J. Capel, S.Y. Park, C. Ra, T. Saito, J.S. Verbeek, J. G. van de Winkel, FcR gamma-chain is essential for both surface expression and function of human Fc gamma RI (CD64) in vivo, Blood 87 (1996) 3593–3599.
[33] G. Dekkers, A.E.H. Bentlage, T.C. Stegmann, H.L. Howie, S. Lissenberg-Thunnissen, J. Zimring, T. Rispens, G. Vidarsson, Affinity of human IgG subclasses to mouse Fc gamma receptors, MAbs 9 (2017) 767–773.
[34] H.J. van der Horst, I.S. Nijhof, T. Mutis, M.E.D. Chamuleau, Fc-engineered antibodies with enhanced Fc-effector function for the treatment of B-Cell malignancies, Cancers 12 (2020).
[35] H.S. Sow, H. Benonisson, C. Breukel, R. Visser, O. Verhagen, A.E.H. Bentlage, C. Brouwers, J.W.C. Claassens, M.M. Linssen, M. Camps, T. van Hall, F. Ossendorp, M.F. Fransen, G. Vidarsson, J.S. Verbeek, FcgammaR interaction is not required for effective anti-PD-L1 immunotherapy but can add additional benefit depending on the tumor model, Int. J. Cancer 144 (2019) 345–354.
[36] R. Dahan, E. Sega, J. Engelhardt, M. Selby, A.J. Korman, J.V. Ravetch, FcgammaRs modulate the anti-tumor activity of antibodies targeting the PD-1/PD-L1 Axis, Cancer Cell 28 (2015) 285–295.
[37] P. Bruhns, B. Iannascoli, P. England, D.A. Mancardi, N. Fernandez, S. Jorieux, M. Daëron, Specificity and affinity of human Fcγ receptors and their polymorphic variants for human IgG subclasses, Blood 113 (2009) 3716–3725.
[38] P. Boross, J.H. Jansen, A. Pastula, C.E. van der Poel, J.H. Leusen, Both activating and inhibitory Fc gamma receptors mediate rituximab-induced trogocytosis of CD20 in mice, Immunol. Lett. 143 (2012) 44–52.
[39] P. Boross, N. van Montfoort, D.A. Stapels, C.E. van der Poel, C. Bertens, J. Meeldijk, J.H. Jansen, J.S. Verbeek, F. Ossendorp, R. Wubbolts, J.H. Leusen, FcRgamma-chain ITAM signaling is critically required for cross-presentation of soluble antibody-antigen complexes by dendritic cells, J. Immunol. 193 (2014) 5506–5514.
[40] J. Westman, S. Grinstein, P.E. Marques, Phagocytosis of necrotic debris at sites of injury and inflammation, Front. Immunol. 10 (2019) 3030.
[41] A. Hochreiter-Hufford, K.S. Ravichandran, Clearing the dead: apoptotic cell sensing, recognition, engulfment, and digestion, Cold Spring Harb. Perspect. Biol. 5 (2013), a008748.
[42] S. Walbaum, B. Ambrosy, P. Schutz, A.C. Bachg, M. Horsthemke, J.H.W. Leusen, A. Mocsai, P.J. Hanley, Complement receptor 3 mediates both sinking phagocytosis and phagocytic cup formation via distinct mechanisms, J. Biol. Chem. 296 (2021), 100256.